

DISCOVERY OF TWO HIGH-MAGNETIC-FIELD RADIO PULSARS

F. CAMILO,^{1,2} V. M. KASPI,^{3,4,8} A. G. LYNE,² R. N. MANCHESTER,⁵ J. F. BELL,⁵ N. D'AMICO,^{6,7}
 N. P. F. MCKAY,² AND F. CRAWFORD³

Accepted for publication by The Astrophysical Journal, April 18, 2000

ABSTRACT

We report the discovery of two young isolated radio pulsars with very high inferred magnetic fields. PSR J1119–6127 has period $P = 0.407$ s, and the largest period derivative known among radio pulsars, $\dot{P} = 4.0 \times 10^{-12}$. Under standard assumptions these parameters imply a characteristic spin-down age of only $\tau_c = 1.6$ kyr and a surface dipole magnetic field strength of $B = 4.1 \times 10^{13}$ G. We have measured a stationary period-second-derivative for this pulsar, resulting in a braking index of $n = 2.91 \pm 0.05$. We have also observed a glitch in the rotation of the pulsar, with fractional period change $\Delta P/P = -4.4 \times 10^{-9}$. Archival radio imaging data suggest the presence of a previously uncataloged supernova remnant centered on the pulsar. The second pulsar, PSR J1814–1744, has $P = 3.975$ s and $\dot{P} = 7.4 \times 10^{-13}$. These parameters imply $\tau_c = 85$ kyr, and $B = 5.5 \times 10^{13}$ G, the largest of any known radio pulsar.

Both PSR J1119–6127 and PSR J1814–1744 show apparently normal radio emission in a regime of magnetic field strength where some models predict that no emission should occur. Also, PSR J1814–1744 has spin parameters similar to the anomalous X-ray pulsar (AXP) 1E 2259+586, but shows no discernible X-ray emission. If AXPs are isolated, high magnetic field neutron stars (“magnetars”), these results suggest that their unusual attributes are unlikely to be merely a consequence of their very high inferred magnetic fields.

Subject headings: pulsars: individual (PSR J1119–6127, PSR J1814–1744)

1. INTRODUCTION

The pulsar in the Crab nebula (PSR B0531+21), with period $P = 33$ ms, was born in a type II supernova observed in 1054 AD, supporting the view that at least some core-collapse supernovae (SNe) form pulsars. Based largely on studies of the Crab and a few other young objects, a picture has emerged where pulsars are born spinning rapidly (with initial period $P_0 \approx 20$ ms in the case of the Crab), and spin down due to their large magnetic moments according to $\dot{\nu} \propto -\nu^n$. In this spin-down law $\nu = 1/P$ is the pulsar rotation frequency, $\dot{\nu}$ is its derivative, and $n = \nu\dot{\nu}/(\dot{\nu})^2$ is the “braking index.” Integration of the spin-down law with constant magnetic moment gives the age of the pulsar,

$$\tau = \frac{P}{(n-1)\dot{P}} \left[1 - \left(\frac{P_0}{P} \right)^{n-1} \right]. \quad (1)$$

Braking indices have been measured for only four pulsars, namely PSRs B0531+21, B0540–69, B0833–45, and B1509–58, with values for n of 2.51 ± 0.01 , 2.2 ± 0.1 , 1.4 ± 0.2 , and 2.837 ± 0.001 respectively (Lyne, Pritchard, & Smith 1993; Deeter, Nagase, & Boynton 1999; Lyne et al. 1996; Kaspi et al. 1994). In other cases, an oblique rotating vacuum dipole model is typically assumed, for which $n = 3$ (Manchester & Taylor 1977), and if $P_0 \ll P$, equation (1) reduces to $\tau = P/(2\dot{P}) \equiv \tau_c$, the characteristic age of a pulsar. With a neutron star radius of

10^6 cm and moment of inertia of 10^{45} g cm², the surface magnetic field strength is

$$B = 3.2 \times 10^{19} \sqrt{P\dot{P}} \text{ G}. \quad (2)$$

The luminosity generated in the braking of the pulsar rotation, $\dot{E} = 4\pi^2 I \nu \dot{\nu}$, is emitted in the form of magnetic dipole radiation and a relativistic particle wind. The vast majority of this luminosity may be deposited in the ambient environment, powering a plerionic supernova remnant (SNR) such as the Crab synchrotron nebula, while a very small portion may be observed as pulsed electromagnetic radiation.

Despite the above, many questions remain regarding the outcome of type II SNe and the manifestation of young neutron stars. Although Galactic SNe and pulsar formation rates are both notoriously difficult to estimate (see, e.g., van den Bergh & Tammann 1991; Tammann, Löffler, & Schröder 1994; Woltjer 1998, and Narayan & Ostriker 1990; Lorimer et al. 1993; Lyne et al. 1998), it is quite plausible that type II SNe occur significantly more often than radio pulsars of the kind already known are born (see van den Bergh & Tammann 1991; Woltjer 1998). If this is the case, perhaps some young neutron stars are being “missed.” A possible example is SNR 3C58, the likely outcome of a type II SN observed about 820 yr ago, with no detectable pulsar. Studying the energetics and morphology of the remnant, Helfand, Becker, & White (1995) make a compelling case for the presence of an unseen pulsar with higher magnetic

¹Columbia Astrophysics Laboratory, Columbia University, 550 West 120th Street, New York, NY 10027. E-mail: fernando@astro.columbia.edu

²University of Manchester, Jodrell Bank Observatory, Macclesfield, Cheshire, SK11 9DL, UK

³Department of Physics and Center for Space Research, Massachusetts Institute of Technology, Cambridge, MA 02139

⁴Department of Physics, Rutherford Physics Building, McGill University, 3600 University Street, Montreal, Quebec, H3A 2T8, Canada

⁵Australia Telescope National Facility, CSIRO, P.O. Box 76, Epping, NSW 1710, Australia

⁶Osservatorio Astronomico di Bologna, via Ranzani 1, 40127 Bologna, Italy

⁷Istituto di Radioastronomia del CNR, via Gobetti 101, 40129 Bologna, Italy

⁸Alfred P. Sloan Research Fellow

field than any previously known. Having a short period like the Crab at birth, such a pulsar would have spun down rapidly to a present long period. Maybe yet other pulsars are born spinning slowly and never generate the large \dot{E} required to power an easily detectable nebula. In addition, some neutron stars may never manifest themselves as radio pulsars at all. It has been suggested that there exists a class of isolated rotating neutron stars with ultra-strong magnetic fields, the so-called “magnetars” (Duncan & Thompson 1992). The observational properties of radio pulsars and magnetar candidates are very different. Radio pulsars rarely exhibit X-ray pulsations, and when they do, their X-ray power is small compared to their \dot{E} . By contrast, magnetars emit pulsed X-rays with luminosities far in excess of their spin-down power (Vasisht & Gotthelf 1997; Kouveliotou et al. 1999) but remain undetected at radio wavelengths. The dichotomy is thought to result from the much larger magnetic fields in magnetars (Thompson & Duncan 1993; Heyl & Hernquist 1997).

In this paper we report the discovery of two isolated radio pulsars with some properties that are unusual and interesting in the context of the above questions.

2. OBSERVATIONS AND RESULTS

The radio pulsars J1119–6127 and J1814–1744 were discovered on 1997 August 24 and 23, respectively, in a survey of the Galactic plane using the 64-m Parkes radio telescope in Australia. This survey (Lyne et al. 2000a; Camilo et al. 2000) makes use of the fast rate of sky coverage afforded by a multibeam receiver to increase greatly the integration time, and consequently the sensitivity, relative to previous surveys. The Parkes survey uses 13 beams at a central sky frequency of 1374 MHz with an equivalent system noise of $S_0 = 35$ Jy at high Galactic latitude. For each beam, the sum of two orthogonal linear polarization channels, each 288 MHz wide, is recorded for 35 minutes per grid position, providing sensitivity to all pulsars with flux densities in excess of ~ 0.15 mJy for $P \gtrsim 0.1$ s.

Follow-on regular timing observations have been carried out at Parkes since 1998 February for newly discovered pulsars with declination south of -35° , while the remainder are observed with the 76-m telescope at Jodrell Bank Observatory, England. The system used for timing observations at Parkes is identical to that used in the survey, although we record signals from the central beam only: the down-converted radio-frequency noise is passed through a $2 \times 96 \times 3$ -MHz filter bank spectrometer, after which the signals are square-law detected, orthogonal polarizations are summed, and the 96 resulting voltages are high-pass filtered before being 1-bit digitized every $250 \mu\text{s}$ and written to magnetic tape for subsequent analysis. We also record the start time of each observation, synchronized with the observatory time standard and traceable to UTC. PSR J1119–6127, in whose direction $S_0 = 40$ Jy, was observed in this manner on 63 days over a period of two years, for approximately 10 minutes each day. At Jodrell Bank, with $S_0 = 50$ Jy in the direction of PSR J1814–1744, the observing setup used a $2 \times 32 \times 3$ -MHz filter bank until 1999 July, and a $2 \times 64 \times 1$ -MHz filter bank since then, to observe a band centered in the range 1376 to 1396 MHz, depending on the radio-frequency interference environment. Signals from individual frequency channels are delayed by an amount proportional to the dispersion measure (DM) of the pulsar, to account for dis-

persion caused by propagation through the interstellar medium, and are folded synchronously with the predicted rotation period, generating one pulse profile for each sub-integration lasting 3 minutes. We have observed PSR J1814–1744 in this manner on 37 days over a two-year interval, for 18 minutes each day.

We have analyzed the timing data in standard fashion. Briefly, topocentric pulse times-of-arrival (TOAs) were measured by cross-correlating daily-averaged pulse profiles with a high signal-to-noise-ratio template (see Fig. 1). Celestial coordinates and spin parameters were then determined using the TEMPO software package⁹ and the JPL DE200 planetary ephemeris (Standish 1990). TEMPO first converts the TOAs to the barycenter of the solar system, and refines the initial estimated parameters in a fitting procedure that minimizes timing residuals (difference between observed and predicted TOAs) with respect to the model parameters.

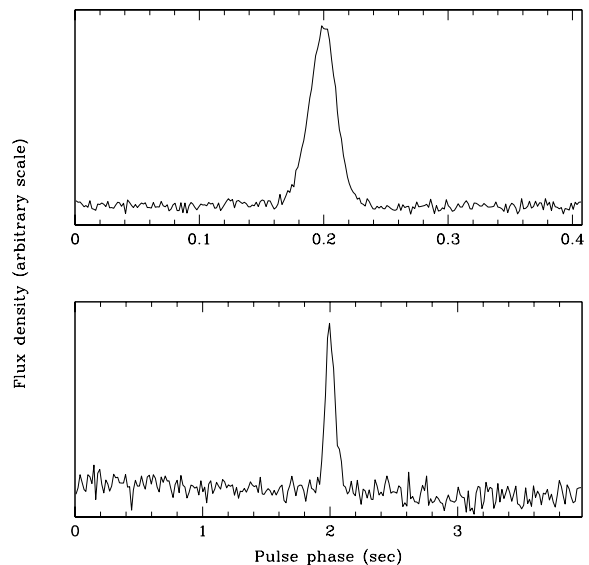


FIG. 1.— Integrated pulse profiles for PSRs J1119–6127 (top) and J1814–1744 (bottom) at a frequency of 1374 MHz.

Underlying the timing model is the assumption that the rotational phase of the neutron star is described by

$$\phi(T) = \nu T + \frac{1}{2} \dot{\nu} T^2 + \frac{1}{6} \ddot{\nu} T^3 + \dots, \quad (3)$$

where T denotes pulsar proper time. In equation (3), the interpretation of ν and its derivatives as representing only the stationary spin parameters of a rotating magnetic dipole does not hold strictly for pulsars displaying rotational irregularities, and parameter estimation in such circumstances must be performed with extra care.

PSR J1119–6127 was observed on 1998 October 30 and 31 with the Australia Telescope Compact Array (ATCA), with the interferometer in its “6D” configuration (Lazendic 1999). The observations were done in pulsar gating mode simultaneously at center frequencies of 1384 and 2496 MHz, with 128 MHz of bandwidth in each of two linear polarizations at each frequency. The radio sources 1934–638 and 1036–697 were used as flux density and phase calibrators, respectively. The data were processed using the MIRIAD package¹⁰, during which on- and off-

⁹<http://pulsar.princeton.edu/tempo>.

¹⁰<http://www.atnf.csiro.au/computing/software/miriad>.

pulse maps were generated. The data set at 1384 MHz, at which frequency the pulsar is brightest, was used to obtain the position of the pulsar, and the 2496 MHz observation was used to determine the flux density, both listed in Table 1.

Because PSR J1119–6127 has the largest period derivative (\dot{P}) of any known radio pulsar, and \dot{P} correlates highly with “timing noise” (Arzoumanian et al. 1994) which can bias the celestial coordinates determined with timing data, we use the position obtained from interferometric observations in the timing solution. We then fit for ν , $\dot{\nu}$, and $\ddot{\nu}$. Figures 2a and b indicate a small glitch in rotation occurred on about MJD 51398; glitch parameters are given in Table 1. Figure 2b also suggests that another glitch of similar magnitude may have occurred sometime during MJD 50850–50940, but we cannot be sure. The rotational parameters best describing the behavior of the pulsar are listed in Table 1, with the corresponding timing residuals shown in Figure 2c.

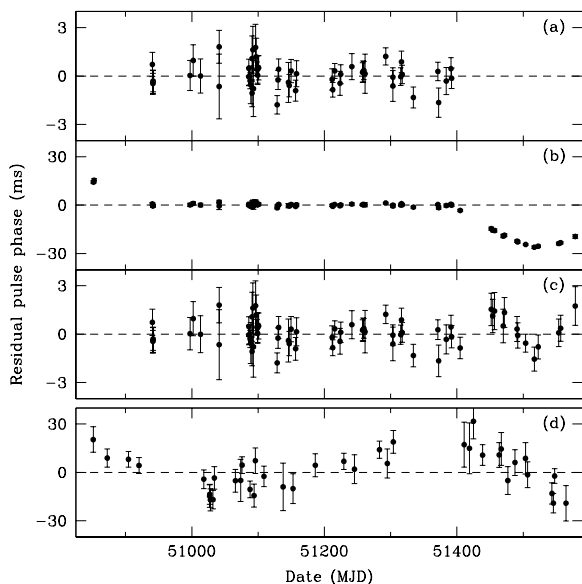


FIG. 2.— (a) Timing residuals for PSR J1119–6127 using data collected over 1998 May–1999 August after fitting for ν , $\dot{\nu}$, and $\ddot{\nu}$. (b) Residuals for entire data set using model obtained in (a), showing a glitch at about MJD 51398. (c) Residuals using data collected over 1998 May–2000 February after fitting for ν , $\dot{\nu}$, $\ddot{\nu}$, and glitch parameters. (d) Post-fit residuals for PSR J1814–1744.

In Figure 2c the residuals following the glitch appear cubic in shape, with amplitude much reduced by comparison with the parabolic residuals in Figure 2b. This suggests that the glitch parameters in Table 1 do not completely describe the behavior of the pulsar following the event. Further data are required to determine whether the post-glitch spin parameters are relaxing with exponential decay time-scales of order several months, as seen in the Vela pulsar, or whether the change in $\dot{\nu}$ at the glitch (or at least much of it) is permanent, as observed in the Crab pulsar (see Lyne, Shemar, & Graham-Smith 2000b).

The uncertainty in the braking index determined from the spin parameters, $n = 2.91 \pm 0.01$, reflects only the random phase noise resulting from uncertainty in the TOAs. We now consider the effect upon this measurement of the possible presence of timing noise and the known occurrence of glitch(es). For most pulsars the stationary value of $\ddot{\nu}$ in equation (3) is too small to be measured, and in timing fits where only ν and $\dot{\nu}$ are determined, excess noise manifests itself as a quasi-cubic trend in

the residuals. Arzoumanian et al. (1994) use the parameter

$$\Delta(t) = \log \left(\frac{1}{6\nu} |\ddot{\nu}| t^3 \right) \quad (4)$$

to estimate the cumulative phase contribution over time t due to timing noise and find that, for $t = 10^8$ s (arbitrary, but similar to the time span of their observations), most pulsars, despite a large scatter in the data, follow the relationship

$$\Delta_8 = 6.6 + 0.6 \log \dot{P}. \quad (5)$$

Using equations (4)–(5) for PSR J1119–6127, we estimate that the measured value of $\ddot{\nu}$ may be contaminated by as much as $8 \times 10^{-24} \text{ s}^{-3}$, or four times the formal uncertainty given in Table 1. In fact we have not measured any timing noise for this pulsar, as indicated by the apparently “white” residuals (Fig. 2a) and by the upper limit on, rather than measurement of, $\ddot{\nu}$ obtained in an additional fit to the data represented in Figure 2a (see Table 1). However this is not too surprising, given that our inter-glitch data span only 1.2 yr; with a longer time span between glitches, timing noise, if it is present, may be measurable. In summary, we believe an accurate measurement of the braking index between glitches, reflecting the steady spin-down physics of the neutron star, is $n = 2.91 \pm 0.01 \pm 0.04$.

If the change in $\dot{\nu}$ at the glitch, $\Delta\dot{\nu}$ (Table 1), is permanent, it contributes a component to $\ddot{\nu}$ beyond that measured between glitches. This contribution is approximately $\Delta\dot{\nu}/\Delta T$, where ΔT is the time interval between glitches. By assuming that all of the measured $\Delta\dot{\nu}$ is permanent, and that a first glitch did occur at MJD ~ 50900 (see Fig. 2b), we obtain $\Delta\ddot{\nu} = -2 \times 10^{-23} \text{ s}^{-3}$, about 10 times the formal uncertainty in $\ddot{\nu}$ and implying a correction to n of -0.1 . Future measurements will settle this question, but for the purposes of calculating pulsar age, the correct value of braking index may be as low as ≈ 2.8 . A similar effect is seen in the Crab pulsar, where permanent changes in spin-down rate occurring at glitches contribute a correction of -0.05 to the value of $n = 2.5$ measured between glitches (Nice 1993).

The quasi-cubic trend in the residuals of PSR J1814–1744 shown in Figure 2d suggests the presence of timing noise in this pulsar. In these circumstances, we determined its position by “whitening” the residuals with a fit of the data to a model incorporating celestial coordinates, ν , $\dot{\nu}$, and $\ddot{\nu}$. We took the resulting coordinates, with uncertainties, as our best unbiased estimate of position, and kept them fixed in subsequent fits to the timing data. We then performed one fit for ν and $\dot{\nu}$, resulting in the best values for these stationary parameters averaged over the data span, with residuals displayed in Figure 2d and showing some red-noise. Finally we performed one extra fit with the additional free parameter $\ddot{\nu}$, which is not stationary. Values obtained for all these parameters are listed in Table 1. We note that the value of $\ddot{\nu}$, an estimate of the amount of timing noise present in PSR J1814–1744, is approximately at the level expected from equations (4)–(5). Note that the uncertainty in declination is particularly large because this pulsar is located at low ecliptic latitude.

The DMs quoted in Table 1 were obtained by folding raw data at the known pulse period for each of four frequency sub-bands, created by the addition of data from 24 adjacent frequency channels, and fitting a time-delay between the sub-bands. This was done for timing data in the case of PSR J1119–6127 and discovery data for PSR J1814–1744. Dispersion measures, together with a model for the Galactic electron density distribution (Taylor & Cordes 1993), are used to

TABLE 1
MEASURED AND DERIVED PARAMETERS FOR PULSARS J1119–6127 AND J1814–1744

	PSR J1119–6127	PSR J1814–1744
Right ascension, α (J2000)	11 19 14.30(2) ^a	18 14 42.94(10)
Declination, δ (J2000)	–61 27 49.5(2) ^a	–17 44 25(19)
Rotation frequency, ν (s ^{–1})	2.4531601130(1)	0.2515197413(3)
Frequency derivative, $\dot{\nu}$ (s ^{–2})	–2.4207996(8) $\times 10^{-11}$	–4.7002(4) $\times 10^{-14}$
Second frequency derivative, $\ddot{\nu}$ (s ^{–3})	6.94(2) $\times 10^{-22}$	3.0(7) $\times 10^{-24}$ ^b
Third frequency derivative, $\ddot{\nu}$ (s ^{–4})	< 10 ^{–30}	...
Epoch (MJD)	51173.0	51200.0
Frequency step at glitch, $\Delta\nu$ (s ^{–1})	1.08(10) $\times 10^{-8}$...
Change in $\dot{\nu}$ at glitch, $\Delta\dot{\nu}$ (s ^{–2})	–9.5(13) $\times 10^{-16}$...
Epoch of glitch (MJD)	51398(4)	...
R.M.S. residual (ms) (white/red)	0.7/ ...	6.3/11.2
Dispersion measure, DM (cm ^{–3} pc)	707(2)	834(20)
Flux density at 1374 MHz, S (mJy)	0.9(1)	0.8(1)
Flux density at 2496 MHz (mJy)	0.44(5) ^a	...
Spin period, P (s)	0.40763747736(2)	3.975831061(5)
Period derivative, \dot{P}	4.022602(2) $\times 10^{-12}$	7.4297(6) $\times 10^{-13}$
Surface magnetic field, B (Gauss)	4.1 $\times 10^{13}$	5.5 $\times 10^{13}$
Characteristic age, τ_c (kyr)	1.6	85
Spin-down luminosity, \dot{E} (erg s ^{–1})	2.3 $\times 10^{36}$	4.7 $\times 10^{32}$
Braking index, n	2.91(1)	...
Distance, d (kpc)	2.4–8	10(2)
Radio luminosity, Sd^2 (mJy kpc ²)	~ 25	~ 80
Galactic longitude, l (deg)	292.15	13.02
Galactic latitude, b (deg)	–0.54	–0.21

NOTE.—Units of right ascension are hours, minutes, and seconds, and units of declination are degrees, arcminutes, and arcseconds. Figures in parentheses represent 1 σ uncertainties in least-significant digits quoted.

^aObtained from interferometric observations (see § 2). Celestial coordinates obtained from a fit to data collected over MJD 50940–51392 are $\alpha = 11^{\text{h}}19^{\text{m}}14^{\text{s}}.24(5)$, $\delta = -61^{\circ}27'49''.8(5)$.

^bThis parameter is not stationary (see § 2 for details).

estimate distances to pulsars. For PSR J1119–6127 the implied distance is $d > 30$ kpc. However, the model does not account for most individual HII regions, and, because the pulsar lies in the direction of the Carina spiral arm, with the likelihood of nearby ionizing population I stars, this distance is assuredly a gross overestimate. We believe it is likely that the pulsar is located between the two line-of-sight crossings of the Carina arm, between $d = 2.4$ and 8 kpc. The distance estimate quoted in Table 1 for PSR J1814–1744 is that obtained from the model of Taylor & Cordes (1993).

The flux densities at 1374 MHz listed in Table 1 were determined by converting the average observed signal strength of the pulsars to a scale calibrated using published flux densities at 1400 MHz for a group of high-DM pulsars, taking into account the variation in sky background temperature.

3. DISCUSSION

3.1. PSR J1119–6127

PSR J1119–6127 has the largest period derivative known among radio pulsars. Partly for this reason it was relatively straightforward to measure a stationary $\dot{\nu}$ with a phase-connected timing solution (i.e., through absolute pulse numbering), only the third pulsar for which this has been possible. The resulting value of braking index is $n = 2.91 \pm 0.05$, including possible contamination by timing noise (see § 2), and is in good agreement with that predicted by a model treating the pulsar as an oblique rotator with a current-starved outer magnetosphere (Melatos 1997). For the four other pulsars for which it has been measured, n ranges between 1.4 and 2.8 (see § 1). That ob-

served braking indices are smaller than 3 can be explained in a variety of ways (see Melatos 1997 for a review), including a kinetic energy-dominated flow at the light cylinder, or an increase in the magnetic moment of the star over time (Blandford & Romani 1988). None of these scenarios are consistent with all the observations (Arons 1992). Measurement of $\ddot{\nu}$ would constrain these possibilities further. At present the upper limit in Table 1 is 30 times the value expected from a simple spin-down law (Blandford & Romani 1988). Whether this can be measured, and how much the measurement of n can be improved with further observations, will depend on the level of timing noise and glitch activity displayed by the pulsar.

Assuming that $P_0 \ll P$, but using the measured values of P , \dot{P} , and n (Table 1) in equation (1), the age of PSR J1119–6127 is 1.7 ± 0.1 kyr, including possible biases due to timing noise and glitches (see § 2). Of course, if the pulsar were born spinning slower, it would be younger. For $P_0 = 0.2$ s, half the present period, the age is 1.2 kyr. In any case it is clear that PSR J1119–6127 is among the very youngest neutron stars known.

Three other pulsars with characteristic ages under 2 kyr are known: the Crab pulsar ($\tau_c = 1.3$ kyr), PSR B1509–58 in G320.4–1.2 ($\tau_c = 1.6$ kyr), and PSR B0540–69 in the Large Magellanic Cloud ($\tau_c = 1.7$ kyr). All three are associated with SNRs. We have searched for evidence of an SNR near PSR J1119–6127. Although none is cataloged (Green 1996), data from the Molonglo Observatory Synthesis Telescope obtained at a radio frequency of 843 MHz (Green et al. 1999) reveal a faint ring of radius 7' centered on the pulsar. This could be the expanding blast wave of the SNR. Its size would imply an

expansion velocity of $\sim 10^4 \text{ km s}^{-1}$, for a distance of 8 kpc and age of 1.6 kyr, reasonable for the blast-wave interpretation if the surrounding medium is of low density and relatively uniform. Additional ATCA data show that the shell has a non-thermal radio spectrum (Crawford et al., in preparation). This possible SNR is also X-ray-bright, with its spectrum described by either a power-law or thermal model, and additional observations are required to further constrain its properties (Pivovarov, Kaspi, & Camilo 2000a). Although the supernova that gave birth to this pulsar occurred in an era in which celestial events were recorded by some civilizations, this explosion may have been too far south and/or too distant or too obscured to have been detected by these observers.

The glitch observed in PSR J1119–6127 is small compared to most glitches in most pulsars, with $\Delta\nu/\nu = (4.4 \pm 0.4) \times 10^{-9}$ (Table 1), but it is of similar fractional size as three of the five glitches observed in the Crab pulsar over 23 years (Lyne et al. 2000b). It remains to be seen whether at least some of the change measured in $\dot{\nu}$ is permanent, as seen in the Crab glitches. Unless we were unreasonably lucky, PSR J1119–6127 glitches more often than the Crab pulsar, but it is curious that its glitches share some characteristics with those of the Crab: while its period and magnetic field are approximately 10 times larger than the Crab’s, its age, and perhaps therefore its internal temperature, are similar.

Finally, we compare the PSR J1119–6127 system with some young pulsar/SNR systems. For ages $\lesssim 2000$ yr, the radio luminosity L_R of a synchrotron nebula (“plerion”) with a central pulsar is a measure of the energy output of the pulsar over its lifetime, due to the relatively long lifetime of the radiating electrons. The plerion X-ray luminosity L_X , on the other hand, reflects the current \dot{E} of the pulsar. For the Crab and PSR B0540–69, $L_X \sim 0.05\dot{E}$, while for PSR B1509–58, $L_X \sim 0.01\dot{E}$ (see Helfand et al. 1995, and references therein). For SNR 3C58, Helfand et al. find that all available data can be reconciled with a (candidate) pulsar having $P \sim 0.2$ s, $\dot{P} \sim 4 \times 10^{-12}$ (parameters similar to those of PSR J1119–6127 — see Table 1), and with $L_X \sim 5 \times 10^{-4}\dot{E}$. For PSR J1119–6127, with a current \dot{E} 200 times smaller than the Crab’s, the limit on plerionic X-ray emission is $L_X \lesssim 10^{-3}\dot{E}$ (Pivovarov et al. 2000a). If PSR J1119–6127 were born with a small period, it would have had a much larger \dot{E} within the past ~ 1700 yr, possibly larger than the Crab’s initially. That energetic past might be reflected in plerionic radio emission near the pulsar, depending on the local environment. A measurement of L_X and L_R may in principle provide information about whether PSR J1119–6127 was born with a rapid spin rate, as commonly assumed for most pulsars, or whether it was born a slow rotator.

3.2. PSR J1814–1744

Figure 3 is a plot of \dot{P} versus P for the radio pulsar population. PSRs J1119–6127 and J1814–1744 are indicated, and we infer $B = 4.1 \times 10^{13}$ and 5.5×10^{13} G respectively, using equation (2). These are the highest magnetic field strengths yet observed among radio pulsars. The pulsars with the next largest values of B are PSRs J1726–3530 ($P = 1.1$ s; $B = 3.7 \times 10^{13}$ G) and J1632–4818 ($P = 0.8$ s; $B = 2.3 \times 10^{13}$ G), also discovered in the multibeams survey¹¹. Prior to this survey the largest value was $B = 2.1 \times 10^{13}$ G for the 2.4 s PSR B0154+61 (Arzoumanian et al. 1994).

Also shown in Figure 3 are the sources usually identified as

¹¹See <http://www.atnf.csiro.au/~pulsar/psr/pmsurv/pmwww/pmpsrs.db>.

magnetars, namely the five anomalous X-ray pulsars (AXPs) and two soft gamma repeaters (SGRs) for which P and \dot{P} have been measured. AXPs are characterized by X-ray periods in the range 5–12 s and extremely rapid spin down (Gotthelf & Vasisht 1998), while the SGRs exhibit occasional enormous bursts of γ -radiation and AXP-like X-ray pulsations during quiescence.

Most models of the radio emission physics (Manchester & Taylor 1977) depend on pair-production cascades above the magnetic poles and hence on the magnitude of the magnetic field. However, at field strengths near or above the so-called “quantum critical field,”

$$B_c \equiv \frac{m_e^2 c^3}{e\hbar} = 4.4 \times 10^{13} \text{ G}, \quad (6)$$

the field at which the cyclotron energy is equal to the electron rest-mass energy, processes such as photon splitting may inhibit pair-producing cascades. It has therefore been argued (Baring & Harding 1998) that a radio-loud/radio-quiet boundary can be drawn on the P – \dot{P} diagram, with radio pulsars on one side, and AXPs and SGRs on the other (see dotted line in Fig. 3).

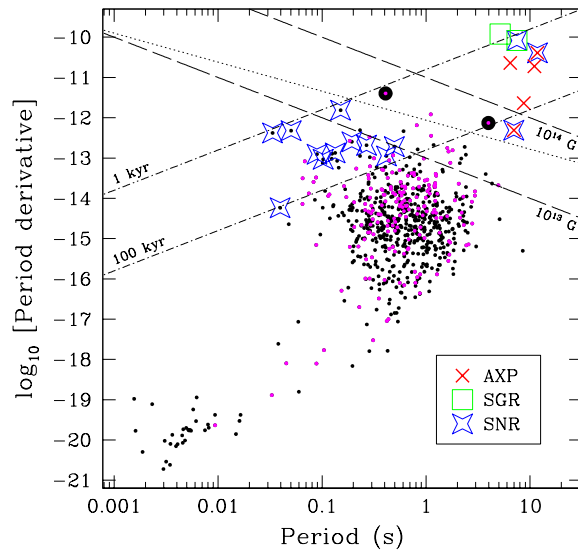


FIG. 3.— Plot of \dot{P} versus P for radio pulsars (dots), anomalous X-ray pulsars (AXPs), and soft gamma-ray repeaters (SGRs). PSRs J1119–6127 and J1814–1744 are identified by large filled circles, and sources plausibly associated with supernova remnants (SNRs) are noted. Lines of constant characteristic age and surface magnetic field strength are drawn. The dotted line shown between the lines for $B = 10^{13}$ and 10^{14} G indicates a hypothesized approximate theoretical boundary (Baring & Harding 1998) separating radio-loud and radio-quiet neutron stars due to effects relating to magnetic fields close to the critical field B_c (see discussion following equation [6]).

The existence of PSRs J1119–6127, J1726–3530, and J1814–1744 demonstrates that radio emission can be produced in neutron stars with $B \gtrsim B_c$. The radio luminosities of these objects (Table 1) are typical for observed radio pulsars. Thus, photon splitting does not appear to inhibit radio emission at these magnetic fields, in agreement with Usov & Melrose (1995) who argue that this process is inhibited by polarization selection rules. Also, there are both astrophysical and instrumental selection effects which bias searches against the detection of long-period ($P \gtrsim 5$ s) radio pulsars such as J1814–1744: evidence suggests their beams are narrower (e.g., Young, Manchester, &

Johnston 1999), so the chances of one intersecting our line-of-sight are smaller, and instrumental high-pass filtering intended to remove baseline variations reduces the sensitivity of searches for such pulsars. Pulsars such as J1814–1744 could therefore be more prevalent than present numbers suggest.

Especially noteworthy is the proximity of PSR J1814–1744 to the cluster of AXPs and SGRs at the upper right corner of Figure 3. In particular, this pulsar has a very similar \dot{P} to that of the well-known AXP 1E 2259+586 (Fahlman & Gregory 1981; Baykal et al. 1998), which has a period of 7 s. The disparity in their emission properties is therefore surprising.

The absence of X-ray emission from the direction of PSR J1814–1744, inferred from archival ASCA and ROSAT observations, implies that it must be significantly less luminous than 1E 2259+586 (Pivovarov, Kaspi, & Camilo 2000b).

The radio emission upper limit for 1E 2259+586 (Coe, Jones, & Lehto 1994; Lorimer, Lyne, & Camilo 1998) implies an upper limit on the radio luminosity at 1400 MHz of 0.8 mJy kpc^2 , 10^{-2} that of PSR J1814–1744, assuming a distance of 4 kpc (Rho & Petre 1997). This limit is comparable to the lowest values observed for the radio pulsar population (Tauris et al. 1994). That the radio pulse may be unobservable because of beaming cannot of course be ruled out.

The radio-loud/radio-quiet boundary line displayed in Figure 3 is more illustrative than quantitative (Baring & Harding 1998). However, the apparently normal radio emission from PSRs J1119–6127, J1726–3530, and J1814–1744, and the absence of radio emission from 1E 2259+586, located very close to PSR J1814–1744 on a P – \dot{P} diagram (Fig. 3), suggests that it may be difficult to delineate any such boundary.

The two sources are also similar in their levels of rotational stability, at least on time scales of ~ 2 yr: PSR J1814–1744 displays timing noise in the amount expected for a radio pulsar with its \dot{P} (see § 2), as is the upper limit on timing noise for 1E 2259+586 over a 2–3 yr span (Kaspi, Chakrabarty, & Steinberger 1999). However, longer term incoherent timing of 1E 2259+586 has revealed significant deviations from a simple spin-down model. These have been interpreted as being evidence for radiative precession of the neutron star, due to its physical distortion by the strong magnetic field (Melatos 1999). Alternatively, Heyl & Hernquist (1999) suggest the deviations are due to extremely large glitches. In either model, similar be-

havior might be expected of PSR J1814–1744; continued radio timing will be sensitive to it.

The similar spin parameters for these two stars and, in turn, many common features between 1E 2259+586 and some other AXPs and SGRs, suggest that very high inferred magnetic field strengths cannot be the sole factor governing whether or not an isolated neutron star is a magnetar or a radio pulsar. Other possible factors include heavy-element atmospheric composition and youth (Thompson & Duncan 1993; Heyl & Hernquist 1997; see also Pivovarov et al. 2000b). The age of PSR J1814–1744, if $P_0 \ll P$ and $n = 3$, is 85 kyr. It is unlikely that any associated supernova remnant would still be observable and indeed there is none known in the vicinity (Green 1996).

We also note that the recently proposed accretion model for AXPs (Chatterjee, Hernquist, & Narayan 2000), in which they are accreting from a fall-back disk formed from material remaining after the supernova explosion, is challenged by PSR J1814–1744. In this model, the neutron star should not be a radio pulsar, but rather an AXP progenitor in a “dim propeller phase,” its rotational frequency being still too high for the accreting material to overcome the centrifugal barrier. Of course, it is always possible that in this one case no fall-back disk formed.

Proof that AXPs or SGRs are isolated high-magnetic-field neutron stars would come from either the discovery of magnetar-like emission from a radio pulsar, or radio pulsations from a putative magnetar. While such radio emission was not expected due to theoretical considerations, because of the high inferred magnetic fields, the discovery of PSR J1814–1744 shows that this emission does occur at magnetic field values characteristic of at least some magnetars, opening the possibility that magnetars also emit observable radio waves.

We thank B. Gaensler for assistance with the MOST data analysis, and D. Nice, M. Pivovarov, D. Helfand, L. Hernquist, and B. Schaefer for useful discussions. The Parkes radio telescope is part of the Australia Telescope which is funded by the Commonwealth of Australia for operation as a National Facility managed by CSIRO. V. M. K. and F. Crawford are supported by a National Science Foundation CAREER award (AST-9875897). F. Camilo is supported by NASA grant NAG 5-3229.

REFERENCES

- Arons, J. 1992, in *The Magnetospheric Structure and Emission Mechanisms of Radio Pulsars*, IAU Colloquium 128, ed. T. H. Hankins, J. R. Rankin, & J. Gil, (Zielona Góra, Poland: Pedagogical University Press), 56
- Arzoumanian, Z., Nice, D. J., Taylor, J. H., & Thorsett, S. E. 1994, *ApJ*, 422, 671
- Baring, M. G. & Harding, A. K. 1998, *ApJ*, 507, L55
- Baykal, A., Swank, J. H., Strohmayer, T., & Stark, M. J. 1998, *A&A*, 336, 173
- Blandford, R. D. & Romani, R. W. 1988, *MNRAS*, 234, 57P
- Camilo, F. et al. 2000, in *Pulsar Astronomy - 2000 and Beyond*, IAU Colloquium 177, ed. M. Kramer, N. Wex, & R. Wielebinski, (San Francisco: Astronomical Society of the Pacific), 3, astro-ph/9911185
- Chatterjee, P., Hernquist, L., & Narayan, R. 2000, *ApJ*. Submitted, astro-ph/9912137
- Coe, M. J., Jones, L. R., & Lehto, H. 1994, *MNRAS*, 270, 178
- Deeter, J. E., Nagase, F., & Boynton, P. E. 1999, *ApJ*, 512, 300
- Duncan, R. C. & Thompson, C. 1992, *ApJ*, 392, L9
- Fahlman, G. G. & Gregory, P. C. 1981, *Nature*, 293, 202
- Gotthelf, E. V. & Vasisht, G. 1998, *New Astr.*, 3, 293
- Green, A. J., Cram, L. E., Large, M. I., & Ye, T. 1999, *ApJS*, 122, 207
- Green, D. A. 1996, in *Supernovae and Supernova Remnants*, IAU Colloquium No. 145, ed. R. McCray & Z. Wang, (Cambridge: Cambridge University Press), 419
- Helfand, D. J., Becker, R. H., & White, R. L. 1995, *ApJ*, 453, 741
- Heyl, J. S. & Hernquist, L. 1997, *ApJ*, 489, L67
- Heyl, J. S. & Hernquist, L. 1999, *MNRAS*, 304, L37
- Kaspi, V. M., Chakrabarty, D., & Steinberger, J. 1999, *ApJ*, 525, L33
- Kaspi, V. M., Manchester, R. N., Siegman, B., Johnston, S., & Lyne, A. G. 1994, *ApJ*, 422, L83
- Kouveliotou, C. et al. 1999, *ApJ*, 510, L115
- Lazendic, J. S. 1999, *Australia Telescope Compact Array User's Guide*, (Sydney: ATNF)
- Lorimer, D. R., Bailes, M., Dewey, R. J., & Harrison, P. A. 1993, *MNRAS*, 263, 403
- Lorimer, D. R., Lyne, A. G., & Camilo, F. 1998, *A&A*, 331, 1002
- Lyne, A. G. et al. 2000a, *MNRAS*, 312, 698
- Lyne, A. G. et al. 1998, *MNRAS*, 295, 743
- Lyne, A. G., Pritchard, R. S., Graham-Smith, F., & Camilo, F. 1996, *Nature*, 381, 497
- Lyne, A. G., Pritchard, R. S., & Smith, F. G. 1993, *MNRAS*, 265, 1003
- Lyne, A. G., Shemar, S. L., & Graham-Smith, F. 2000b, *MNRAS*. In press
- Manchester, R. N. & Taylor, J. H. 1977, *Pulsars*, (San Francisco: Freeman)
- Melatos, A. 1997, *MNRAS*, 288, 1049
- Melatos, A. 1999, *ApJ*, 519, L77
- Narayan, R. & Ostriker, J. P. 1990, *ApJ*, 352, 222
- Nice, D. J. 1993, in *Isolated Pulsars*, ed. K. A. van Riper, R. Epstein, & C. Ho, Cambridge, 391
- Pivovarov, M. J., Kaspi, V. M., & Camilo, F. 2000b, *ApJ*, 535. In press, astro-ph/0001091

Pivovarov, M. J., Kaspi, V. M., & Camilo, F. 2000a, ApJ. In preparation
Rho, J. & Petre, R. 1997, ApJ, 484, 828
Standish, E. M. 1990, A&A, 233, 252
Tammann, G. A., Löffler, W., & Schröder, A. 1994, ApJS, 92, 487
Tauris, T. M. et al. 1994, ApJ, 428, L53
Taylor, J. H. & Cordes, J. M. 1993, ApJ, 411, 674
Thompson, C. & Duncan, R. C. 1993, ApJ, 408, 194

Usov, V. V. & Melrose, D. B. 1995, Aust. J. Phys., 48, 571
van den Bergh, S. & Tammann, G. A. 1991, Ann. Rev. Astr. Ap., 29, 363
Vasisht, G. & Gotthelf, E. V. 1997, ApJ, 486, L129
Woltjer, L. 1998, in The Relationship Between Neutron Stars and Supernova
Remnants, volume 69, Memorie della Società Astronomica Italiana, 1079
Young, M. D., Manchester, R. N., & Johnston, S. 1999, Nature, 400, 848